

**Ferhat Sime**

Mersin University, ferhatsime04@gmail.com, Mersin-Türkiye

Zehra Ordu

Mersin University, z.ordu02@gmail.com, Mersin-Türkiye

Mohammed Abdul-Fattah SalehNational Agricultural Research Center, muh.saleh89@gmail.com,
Cenin-Palestine**Mutlu Yalvaç**

Mersin University, myalvac@mersin.edu.tr, Mersin-Türkiye

DOI	http://dx.doi.org/10.12739/NWSA.2023.18.4.1A0487	
ORCID ID	0000-0002-4925-5982	0000-0003-3964-1203
	0000-0002-3145-4457	0000-0002-1281-5712
Corresponding Author	Zehra Ordu	

REMOVAL OF MALACHITE GREEN DYE FROM AQUEOUS SOLUTION USING *Verbascum Thapsus L.***ABSTRACT**

Humans are the only producers of wastes accumulated in nature. Treatment technologies are developing by following, analyzing and imitating nature. Herbal bioadsorbents are natural substances used in wastewater treatment. In this study, Malachite Green (MG) was removed from the water with *Verbascum Thapsus L.* (VTL). VTL collected from Mount Ararat is a wild and invasive plant. SEM, BET and FTIR were used to determine adsorbent characterization. Experimental design was made with the surface response method (RSM). Optimum values obtained as a result of experimental studies: Adsorbent mass is 0.75g, pH6.5, initial concentration of adsorbed substance is 304mg/L and contact time of adsorption is 40 minutes. It was determined that the adsorption process was carried out in accordance with the Langmuir isotherm ($R^2=0.9997$) and the second-order kinetic model ($R^2=0.9997$). The maximum adsorbent capacity is 38.85 mg/g and the dye removal efficiency is 95%. As a result of the thermodynamic study; Gibbs free energy (ΔG) was found to be negative for all temperatures. According to the results obtained at the end of the study, it was found that VTL is an effective adsorbent that can be used in chemical adsorption to remove MG from aqueous solution.

Keywords: Adsorption, *Verbascum Thapsus L.* (VTL), Surface Response Method (RSM) Malachite Green, Bioadsorbent

1. INTRODUCTION

Water is the most important part of the living body. It is the source of life for people. Not only for life, but also for the environment, agriculture, industry, etc. It is also very important for production. Inorganic and organic wastes generated as a result of human activities cause high amounts of water pollution. These waters pose a threat to human health and other living things [1]. Water pollution attracts attention as a social problem because it causes the destruction of natural ecosystems. Historically, soil and water pollution has been addressed by environmental politicians. However, in order to protect agricultural production and human health, integrated policies that address both soil and water pollution need to be established [3, 4 and 5]. The textile industry accounts for two-thirds of the total dyestuff

How to Cite:

Sime, F., Ordu, Z., Saleh, M.A., and Yalvaç, M., (2023). Removal of Malachite Green Dye From Aqueous Solution Using *Verbascum Thapsus L.*, 18(4):55-71, DOI: 10.12739/NWSA.2023.18.4.1A0487.



market [6]. Dyed wastewater bodies; It is widely produced and applied in cosmetics [7], leather fabric, dyeing process [8], printing house, printing house, dye production and food factories [9]. These wastewaters are pollutants that are difficult to treat and are improperly transported from various sources and discharged directly into water resources [10] [11].

Dyed wastewater discharged into the aquatic environment increases the color saturation of the receiving water [12], prevents sunlight from entering the water, and this disrupts the photosynthesis of aquatic plants [13]. Wastewater poses a serious threat to the ecosystem and people. As a result, dyes are harmful even at very low concentrations [14]. It must be removed from the wastewater through an effective treatment process before it is discharged. Different methods are used to remove dyes from water. For color removal in the literature; Various purification processes have been developed, such as adsorption [15], membrane filtration [16], photocatalytic process [17], electrochemical method [18], advanced oxidation processes [19]. These techniques include adsorption and activity simplicity [20]. It has a great decontamination potential due to its low cost [21], high activity [22], rapid adsorption [23], and the use of a wide variety of adsorbents [15]. It is a promising method due to its many advantages and is widely used. Dye adsorption largely depends on adsorbents. Various studies have been conducted in the field of wastewater treatment using activated charcoal and other commercially available adsorbents. Activated carbon is a preferred material as an adsorbent due to its large surface area, porous structure and diversity of functional groups in its chemical structure. However, such products have not been adopted sufficiently due to the cost of their use [24 and 25]. In recent years, the use of bioadsorbents in adsorption technologies has increased due to their cheap and easy availability. Examples of bioadsorbents used are chitosan, peat, wood, sawdust and agricultural waste [26]. Such adsorbents are low-cost [27], environmentally friendly [28], and inherently safe [29]. According to the latest research; The accessibility and natural availability of the adsorbent [30] make adsorption a promising method [24 and 31].

In this study, it was aimed to adsorb *Verbascum thapsus* L. (VTL) and Malachite green (MG) dyes obtained from Ağrı province. MG is a cationic textile dye widely used in the paper, leather, wool, silk, textile and food industries. Despite its widespread use, it has negative effects on human health [32 and 33]. *Verbascum thapsus* L. (VTL), also known as mullein, is the largest genus of the Scrophulariaceae family with approximately 360 species, often growing in abandoned fields and meadows [34 and 35]. Its homeland is Europe, Asia and North Africa [36]. It is used in the treatment of asthma, cough and migraine [37]. In this study, VTL will be evaluated as a natural, renewable and low-cost material [38]. In this study, it is aimed to adsorb MG dyestuff using VTL facility. There is no adsorption study with VTL in the literature.

2. RESEARCH SIGNIFICANCE

In this study, the adsorption process occurred spontaneously. The maximum adsorption capacity of VTL reached 38.85 mg/g and its efficiency reached 95%. As a result of this process, there is no carbon release into nature. VTL is an adsorbent suitable for combustion after adsorption in cement factories. In this way, it can be evaluated within the scope of zero waste production. Since it is used raw, it does not release carbon into nature, and its use in factories after processing explains the importance of this research.

Highlights:

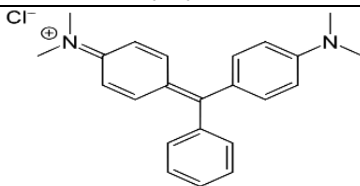
- A wild and invasive plant, *Verbascum Thapsus* L., was used to extract the Malachite Green dye from the aqueous solution

- Bioadsorbents do not release carbon when used untreated
- In VTL adsorption, the maximum adsorption capacity reached 38.85mg/g and the yield reached 95%.

3. MATERIAL AND METHOD

Verbascum thapsus L. (Bovine tail) was used as adsorbent in this study. The VTL used was obtained from rural areas of Ağrı and stored in the refrigerator at +4°C. Malachite green was used as dyestuff in the study.

Table 1. Properties of Malachite Green dyestuff [39 and 40]

Malachite Green	
Molecular weight (g/mol)	364.90
Color	Green
λ_{max} (nm)	619
Purity	<90%
Chemical formula	$C_{23}H_{25}ClN_2$
Chemical structure	

3.1. *Verbascum thapsus* L. (VTL) Preparation

The VTL plant collected from the rural areas of Ağrı province was kept at room temperature (25°C) throughout the studies. The VTL was first washed with tap water. Then VTL was washed with distilled water again and dried in an oven at 105°C for 1 day (24 hours). The dried VTL was passed through a 35 mesh sieve and used as an undersieve bioadsorbent.



Figure 1. *Verbascum Thapsus* L. (VTL)

3.2. Adsorption Experiments

ISOLAB precision balance for weighing MG and VTL in adsorption experiments, MIKROTEST-ELEKTROFOREST shaker incubator to mix the MG stock solution at constant temperature and 150 rpm throughout the experiments, An ISOLAB pH meter was used to adjust the acid-base level and a MICRO22R-HETTICH ZENTRIFUGEN centrifuge at 6000rpm for 5 minutes to separate the dye and herb in the solution. As a result of the experiments, a UV spectrophotometer (HACH DR-3900) at a wavelength of 617nm was used to determine the color change.

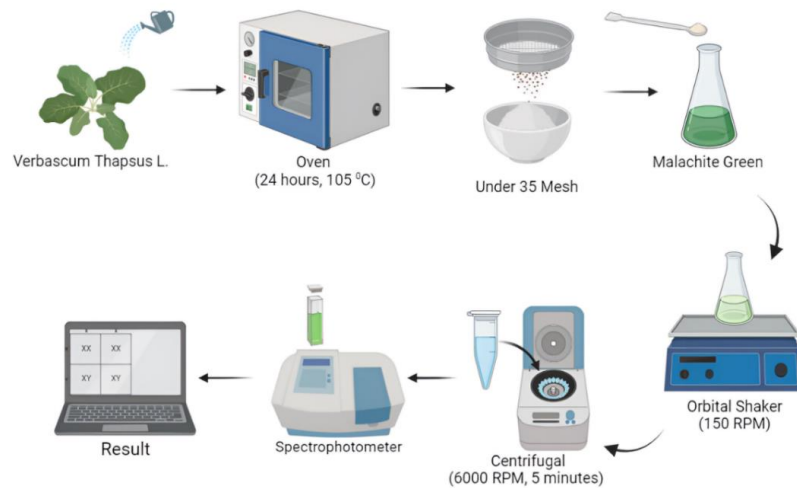


Figure 2. Adsorption experiments

In experiments; Optimization studies of adsorbent mass, pH, initial concentration of adsorbed material, contact time were made by RSM method. Experiments were carried out in 100mL volume and 250mL balloon was used in case of overflow. After the experiment, removal efficiency (%) and adsorbent capacity (q_e) (mg/g) were calculated using formula 1 and formula 2, respectively [4 and 41].

$$\text{Yield } \% = \frac{(C_i - C_f)}{C_i} \times 100 \quad (1)$$

$$q_e = \frac{(C_i - C_f) \times V}{m} \quad (2)$$

m : is defined as the adsorbent mass (g)

C_i : Inlet concentration of MG dye (mg/L)

C_f : Output concentration of MG dye (mg/L)

V : Solution volume (L)

After the adsorption process, dye adsorbent, 0.1 M HCl and 0.1 M NaOH solutions were shaken with different balloons at 150rpm for 24 hours for desorption of MG from VTL. The following equation was used to calculate the percent recovery.

$$\text{Regain } \% = \frac{\text{Desorption Concentration}}{\text{Adsorbed Paint Concentration}} \times 100$$

3.2. Response Surface Methodology (RSM)

Removal of MG from solution with VTL was calculated using RSM. Four independent variable factors were used in the calculations. These; adsorbent mass, pH, initial concentration of adsorbed material and contact time. The number of experiments required to complete the calculations was determined using equation 3 below [42].

$$N = 2^n + 2n + C_p \quad (3)$$

N : Number of experiments to be done

n : Independent number

C_p : Copies of center point numbers.

Independent factor ranges were entered into the established model. The ranges of independent variables are shown in Table 2 (a total of 30 experiments were performed). Experiment results were re-entered into the model. In this study, the Design Expert 11 program was used.

Table 2. Variables to consider and limit values

Variables	Unit	Factor	Highest Value	Low Value
pH	-	A	2	10
VTL mass	g	B	0,1	1
Time	min	C	5	60
MG concentration	mg/L ⁻¹	D	10	400

3.2. Adsorbent Characterization

In determining the surface morphology (VTL) of adsorbents; Scanning Electron Microscopy (SEM), in determining the surface area; Brunauer, Emmett and Teller (BET) and in the measurement of infrared spectra; Fourier Transform Infrared Spectroscopy (FTIR) devices were used.

4. FINDINGS AND DISCUSSION

4.1. Verbascum Thapsus Characterization (VTL)

The formations in the surface morphology of the VTL plant used in experimental studies. SEM (Scanning Electron Microscopy) to study surface area, Brunauer Emmett and Teller (BET) and analysis of the incoming structure of the VTL and functional group FT-IR (Fourier Transform Infrared Spectroscopy) device for analysis used.

4.2. Scanning Electron Microscope (SEM)

SEM imaging was performed to examine and see the changes in the surface morphology of the VTL plant used in the study before and after the adsorption process. The surface morphology of the VTL indicates the presence of irregularly shaped particles of different sizes, as revealed by SEM. SEM images of the VTL are shown in Figure 3.

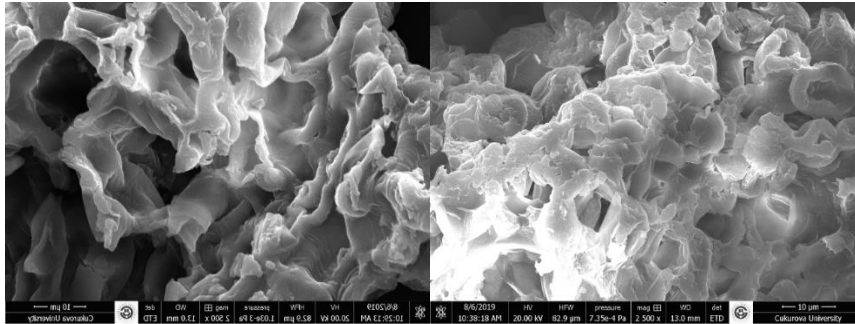


Figure 3. SEM images of the VTL (10x) before and after adsorption

In the examined SEM images, it is possible to see that the dyestuff adheres to the VTL before and after adsorption. Looking at the surface structure of the VTL, it is seen that there are wide indentations. Its wide and wide recesses allow it to interact with the dyestuff in a short time. Thanks to this feature, it reduces the adsorption time. After the adsorption process, it is possible to see that the surface of the VTL is coated with dyestuff.

4.3. Surface Area Measurement (SEM)

In this study, surface areas were determined with BET and Langmuir for the VTL plant. Raw BET and Langmuir surface areas of the VTL; decreases after adsorption. BET and Langmuir plots of raw and dyed VTL are given in Figures 4a, 4b and figures 5a, 5b.

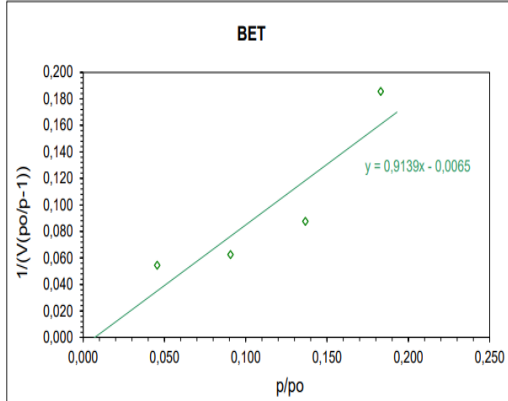


Figure 4a. BET chart for raw VTL

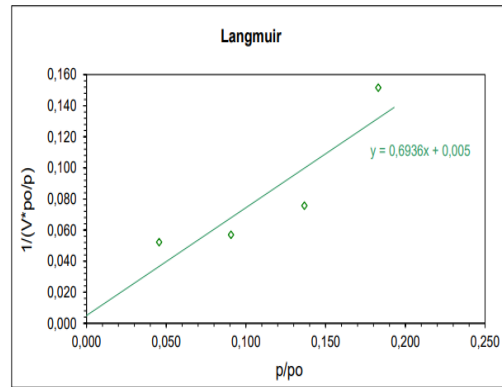


Figure 4b. Langmuir chart for raw VTL

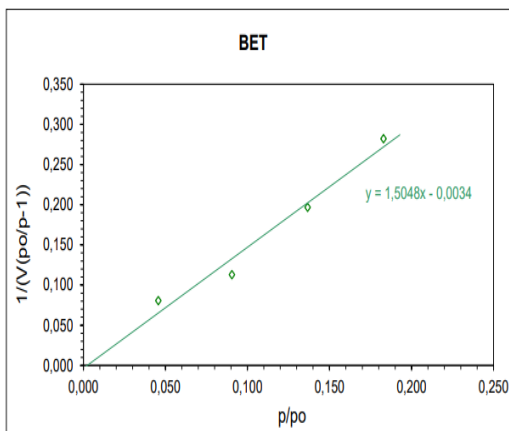


Figure 5a. BET chart for painted VTL

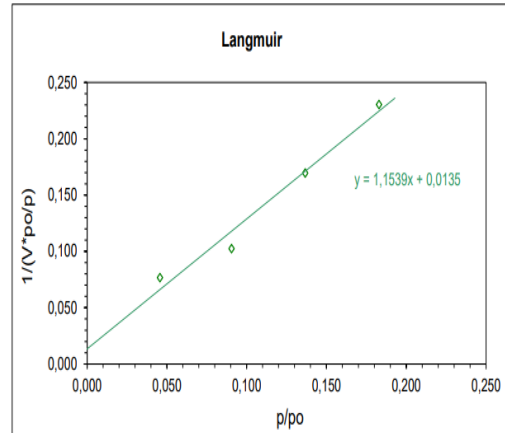


Figure 5b. Langmuir chart for painted VTL

Table 3. Raw and painted BET and Langmuir surface areas of the VTL plant

	VTL Plant	
	Raw	Painted
BET Surface Area (m ² /g)	4.84	2.29
Langmuir Surface Area (m ² /g)	6.33	3.80

4.4. Fourier Transform Infrared Spectroscopy (FT-IR)

FT-IR device in the study; It was used to determine the functional groups in the structure of VTL used as adsorbent. A diagram is created by using the frequencies formed as a result of vibration in determining the functional groups. Spectra are formed in regions where the relevant functional groups are located. Since spectra are specific to substances, it is possible to find functional groups from the resulting spectra. FT-IR analysis of raw and dyed VTL is shown in Figure 6 and 7. According to the FT-IR analysis results, when looking at Figure 6 and Figure 7, it was seen that the peaks in the 504.29, 557.33, 593.00, 895.77, 1159.01, 1316.18, 1424.17, 1453.10 and 2319.95cm⁻¹ bands disappeared after the adsorption process. There were transitions in different groups. These are functional group alkyl halides and peak related the peak shifted from 532.26cm⁻¹ to 539.97cm⁻¹. In addition, shifts to nitro compounds with N-O asymmetric tensile bonds, aliphatic amines with C-N tensile bonds and aromatic functional group with C-C tensile bond (in-ring) occurred. Changes in the spectrum before and after the adsorption process may indicate the characteristic of the adsorption process as sorption. This; It means that the MG reacts with the VTL by changing the

structure of the VTL. Considering all these analyzes, it was determined that the dyestuff in the aqueous solution was adsorbed by VTL.

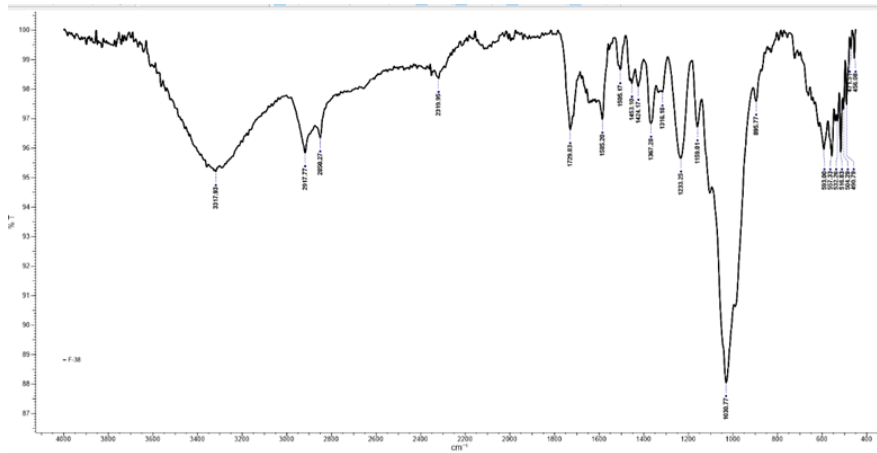


Figure 6. FT-IR Analysis of VTL Before Adsorption Process

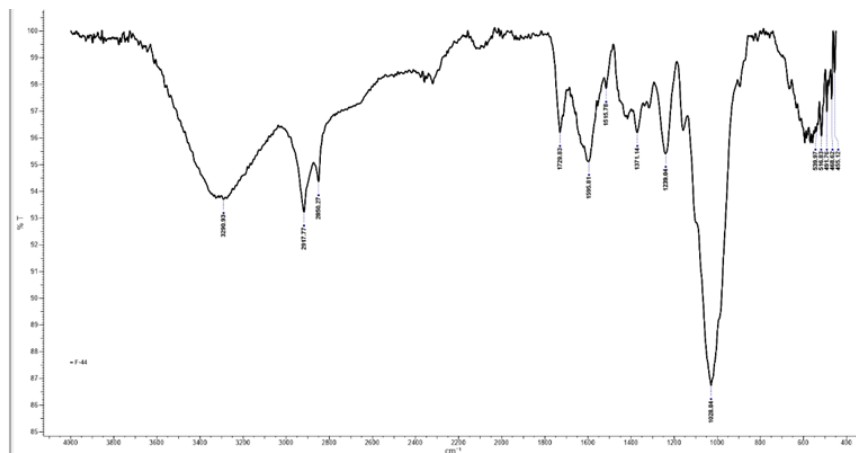


Figure 7. FT-IR Analysis of VTL After Adsorption Process

4.5. Adsorption Optimization

4.5.1. Response Surface Methodology (RSM)

As shown before, the effect of pH (A), time (B), adsorbent (C) and MG (D) concentration on adsorbent capacity was investigated by CCD method. Experimental design and response values are shown in Table 4. When the response values are examined in these studies, it varies between 1.28364-55. The ratio between the maximum and minimum values was calculated as 42,847. Using 2FI, linear, quadratic and cubic models, a representative model with this value greater than 10 and indicating the need for transformation was obtained. According to the regression coefficient value (R^2), the quadratic model, 20 constant values were used to represent the model. Statistical results obtained using the square root method are given in Table 5. The estimated R^2 (0.8056) is in acceptable agreement with the adjusted R^2 (0.9328). So the difference is less than 0.2. Adequate sensitivity measures the signal-to-noise ratio and it is desirable that this ratio be greater than 4. In this study, the ratio was calculated as 20,963, indicating an adequate signal.



Table 4. Experimental design and response values

Std	Set	Variable 1 A:pH	Variable 2 B:Time (min)	Variable 3 C:Adsorbent (g)	Variable 4 D:Concentration (mg/L)	Reaction 1 q mg/g
13	1	4	18.75	0.775	278.1	27.6258
21	2	6	32.50	0.1	141	50.8
5	3	4	18.75	0.775	101.6	11.0968
28	4	6	32.50	0.55	128.4	19.6
2	5	8	18.75	0.325	98.6	18.6362
26	6	6	32.50	0.55	128.4	19.6
16	7	8	46.25	0.775	280.2	32.929
25	8	6	32.50	0.55	128.4	19.6
12	9	8	46.25	0.325	280.5	55
11	10	4	46.25	0.325	279.3	48.9538
6	11	8	18.75	0.775	97.8	9.52258
4	12	8	46.25	0.325	98.6	22.5
22	13	6	32.50	1	136	12.19
24	14	6	32.50	0.55	302.4	43.8364
30	15	6	32.50	0.55	128.6	19.6364
1	16	4	18.75	0.325	93	16.2769
15	17	4	46.25	0.775	278.1	31.4194
29	18	6	32.50	0.55	278.1	44.2727
20	19	6	60.00	0.55	278.1	46.8818
27	20	6	32.20	0.55	195.6	31.8182
14	21	8	18.75	0.775	280.2	28.929
18	22	10	32.50	0.55	195.6	27
3	23	4	46.25	0.325	93	20
9	24	4	18.75	0.325	279.3	38.4923
10	25	8	18.75	0.325	280.5	37
7	26	4	46.25	0.775	101.6	12.271
17	27	2	32.50	0.55	163.4	7.05455
23	28	6	32.50	0.55	7.42	1.28364
19	29	6	5.00	0.55	128.6	13.6364
8	30	8	46.25	0.775	97.8	11.8452

Table 5. Statistical results obtained using the square root method

Source	Std. Dev.	R ²	Adjusted R ²	Estimated R ²	PRESS	
Lineer	0.3915	0.8822	0.8633	0.8190	5.89	Suggested
2FI	0.4303	0.8918	0.8349	0.7743	7.34	-
Kuadratik	0.2746	0.9652	0.9328	0.8056	6.32	Suggested
Kübik	0.0375	0.9998	0.9987	-	-	Aliased

4.5.2. Effects of Parameters

As shown in the equation, the relationship between the adsorbent mass of VTL, pH, initial concentration of adsorbed material and contact time was investigated.

$$\begin{aligned}
 &\sqrt{\text{capacity}} + 20 \\
 &= 3.2634469422279 + 0.7361910085515 \text{ pH} + 0.030576144160436 \text{ Time} \\
 &- 3.8320691732475 \text{ Mass} + 0.014625739910759 \text{ Concentration} \\
 &+ 0.0012771378658366 \text{ pH} \times \text{Time} - 0.054483712362636 \text{ pH} \times \text{Mass} \\
 &+ 0.000020365506371925 \text{ pH} \times \text{Concentration} \\
 &- 0.030679433759497 \text{ Time} \times \text{Mass} + 0.000070127350927879 \text{ Time} \\
 &\times \text{Concentration} - 0.00022050480936681 \text{ Mass} \times \text{Concentration} \\
 &- 0.057007635936358 \text{ pH}^2 - 0.0002920354480329 \text{ Time}^2 \\
 &+ 2.6811977780878 \text{ Mass}^2 - 0.000019152731287654 \text{ Concentration}^2
 \end{aligned}$$

4.5.3. Model Optimization

The developed model is optimized to determine the optimum conditions. For the optimization process, the pH (4-8) contact time was chosen as (18.75-45.00) minutes, respectively. A "minimum" amount of adsorbent dose and "maximum" dye concentration are recommended to reach

the maximum adsorbent value. Optimum variable values are given in Table 6.

Table 6. Model optimization values

pH	Time (min)	Adsorbent (g)	Dye Concentration (mg/L)	Adsorption Capacity (mg/g)
6.50	40.00	0.75	304.00	38.85

4.5.4. Effect of Independent Factors on Capacity

The adsorption process takes place in the pH range of 4-8. However, the maximum adsorption capacity was obtained in the pH range of 6.38 to 7.28 as shown in Figure 8.

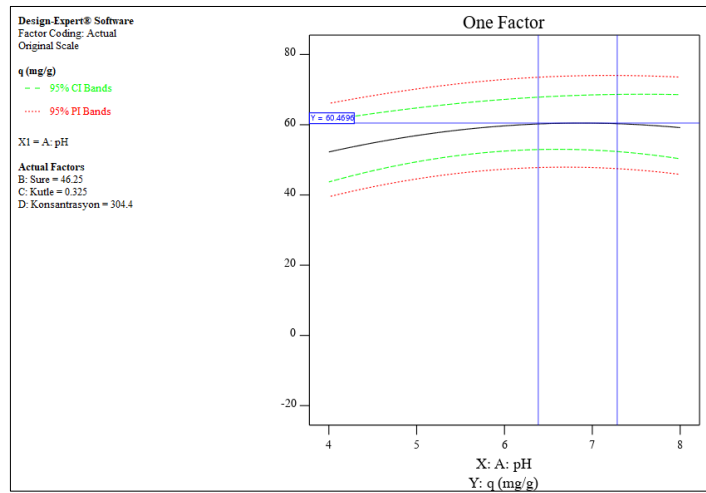


Figure 8. Effect of pH on adsorption capacity

As the contact time increases, the adsorption capacity increases. The change in contact time and adsorption capacity depending on pH is shown in Figure 9. The maximum adsorption capacity is reached in the pH range of 6.38-7.28. But after 7.28 there is a decrease in pH.

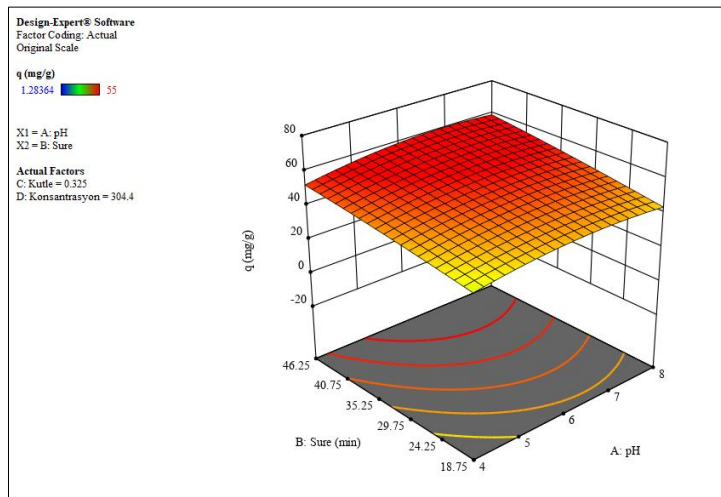


Figure 9. Effect of Time and pH on adsorption capacity

There is an inverse relationship between the mass of the adsorbent and its capacity. MG concentration is directly proportional to capacity. The maximum capacity, mass effect and contact time obtained at minimum mass and maximum concentration are shown in Figure 9.

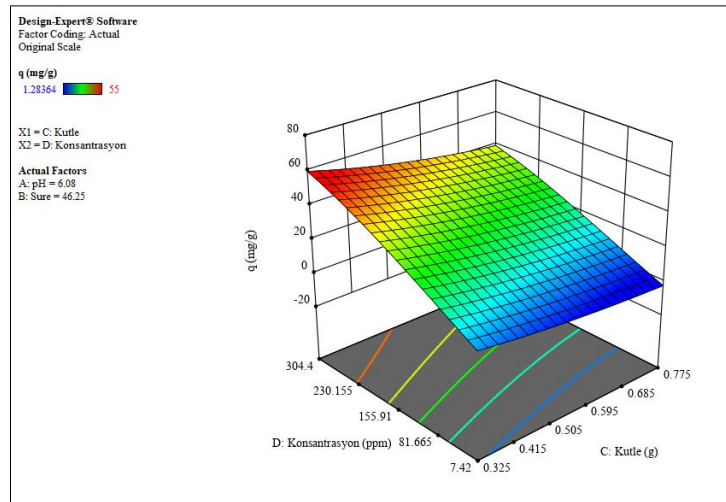


Figure 10. Effect of VTL and MG concentration on adsorption capacity

4.5.5. Adsorption Isotherms

In this study, Langmuir and Freundlich Isotherm models for VTL used as MG dyestuff and adsorbent in aqueous solution were examined separately. The Langmuir Isotherm is created by plotting the change of C_e/q_e against C_e , calculated at equilibrium. The generated graph is shown in Figure 11. The Freundlich Isotherm model is constructed on the graph of the change of $\log q_e$ calculated against $\log C_e$ at equilibrium. The generated graph is shown in Figure 12. The isotherm coefficients calculated using the isotherm graphs given in Figure 11 and Figure 12 are given in Table 7.

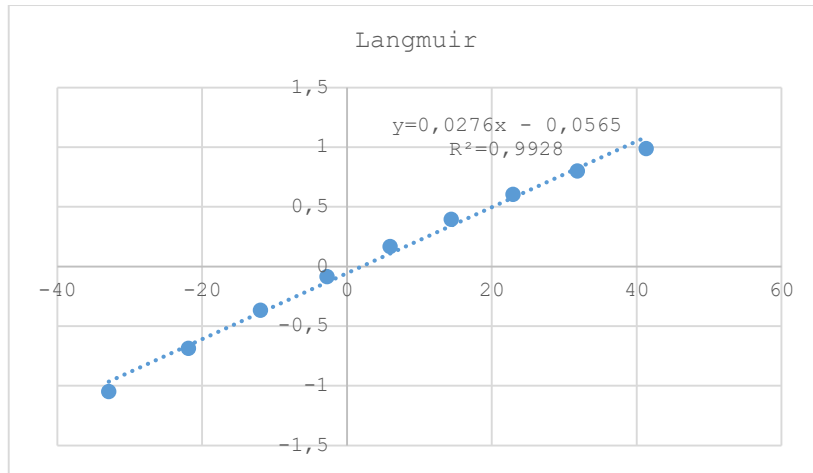
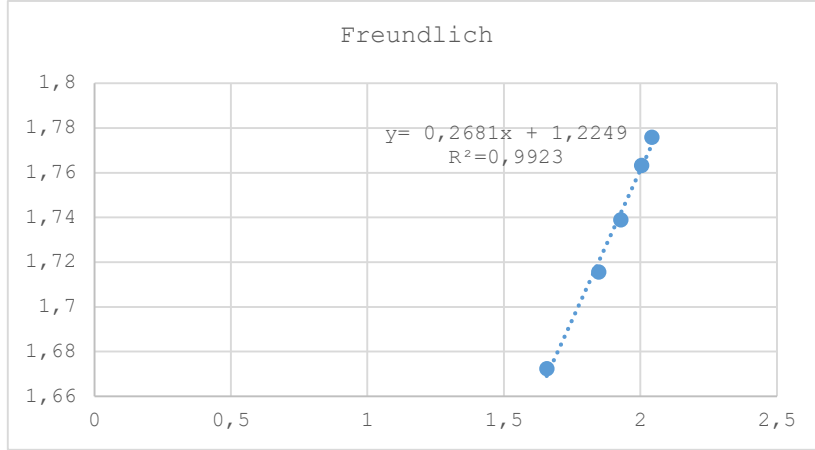


Figure 11. Langmuir isotherm graph



Şekil 12. Freundlich isotherm graph

Table 7. Langmuir and freundlich isotherm constants

	Isotherm Constants
Langmuir Isotherm	$K_L = -1.5493$ $a_L = -0.0351$ $R^2 = 0.9953$ $Q_{max} = 73.53$
Freundlich Isotherm	$K_F = 16.7842$ $n = -7299$ $R^2 = 0.9924$

When Figure 10 and Figure 11 are examined, it is seen that Langmuir Isotherm model is more suitable as a valid isotherm model for adsorbing MG dyestuff in aqueous solution on VTL used as adsorbent. As seen in Table 7, the adsorbent capacity of the VTL was calculated as 73.53mg/g when the Langmuir Isotherm model was applied.

4.6. Adsorption Kinetics

4.6.1. First Order Kinetic Model

In this study, $\log(q_e - q_t)$ vs time (min) graph shown in Figure 13 was created to interpret the change in the rate of change of adsorption capacity over time.

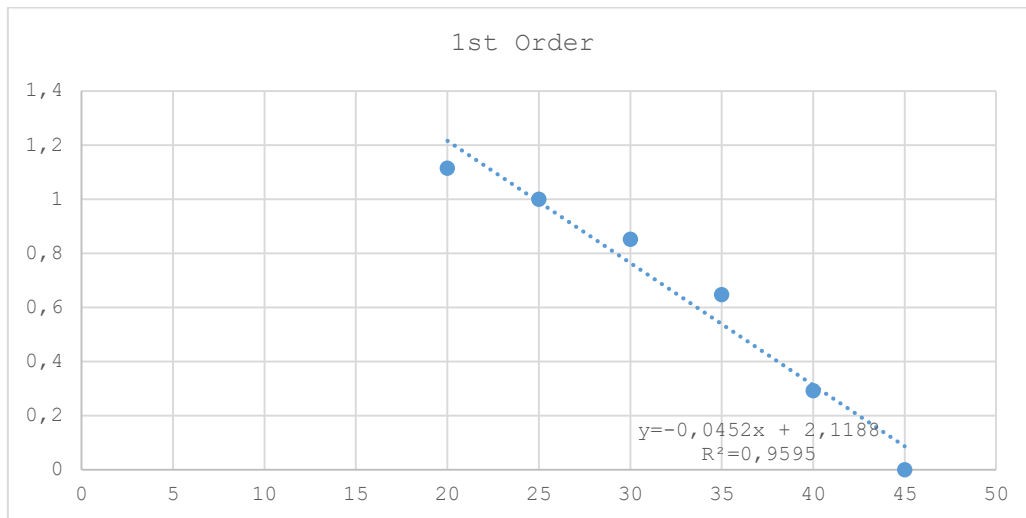


Figure 13. First-order kinetic model (MG-VTL)

4.6.2. Quadratic (Pseudo) Kinetic Model

A t-chart to t/qt was constructed to interpret the time dependent variation of adsorption capacity. The drawn graph is shown in Figure 14.

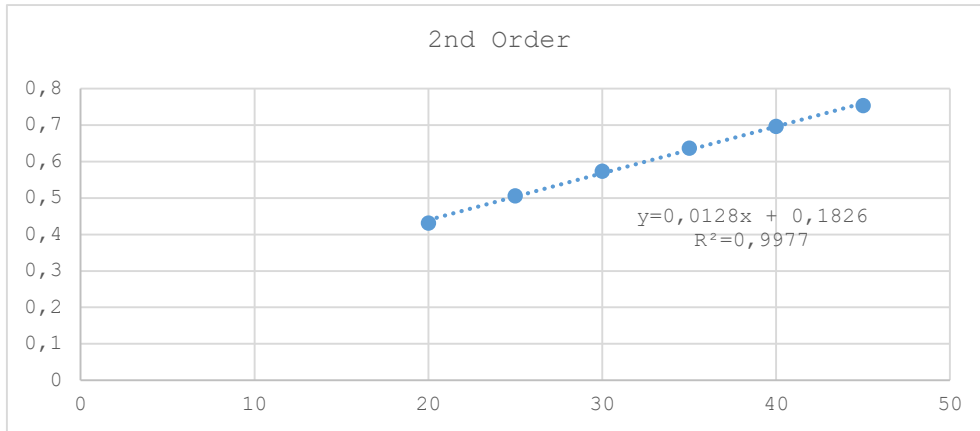


Figure 14. Quadratic (pseudo) kinetic model (MG-VTL)

Considering the R2 numbers (regressions) given in Figure 14, although it is very close to the first-order model, it was determined that the second-order kinetic model was suitable for use in the adsorption of MG to VTL.

4.7. Thermodynamics

Gibbs free energy (ΔG) was found to be negative for all temperatures. This means that the adsorption phenomenon occurs spontaneously. Enthalpy values (ΔH) were found positive. This indicates that adsorption is an endothermic reaction that takes energy in the form of heat. Entropy values (ΔS) were found positive. This indicates that there may be a structural change between the VTL plant and the MG dye.

Table 8. Thermodynamic Studies at Different Temperatures

T (°C)	ΔH (kJ/mol)	ΔS (J/mol.k)	ΔG (kJ/mol)
35	32.714	119.460	-4.081
40			-4.678
50			-5.873

4.8. Desorption

In this study, 5, 15, 35, 60, 90, 120 minutes and 24-hour desorption studies were performed separately in 0.1 M HCl and 0.1 M NaOH in 100 ml volume, and the desorption percentages are given in Table 9. According to the results given in Table 9, the maximum desorption percentages of HCl and NaOH were calculated as 4.04 and 0.41, respectively.

Table 9. Desorption Results with HCl and NaOH Solution

Time (min)	HCl (100 mL)	NaOH (100 mL)	Recovery With HCl (%)	Recovery With NaOH (%)
5	3.12	0.18	2.36	0.15
15	4.78	0.23	3.62	0.19
35	4.70	0.23	3.56	0.19
60	5.06	0.29	3.83	0.24
90	5.02	0.30	3.80	0.25
120	5.15	0.33	3.90	0.28
24 saat	5.34	0.48	4.04	0.41



As a result, considering the factors such as the lack of economic value and easy availability of the *V. thapsus* plant, its use as an adsorbent was found to be suitable for MG dye adsorption. According to the researched data, the highest dye adsorption at room temperature was 304.00mg/L, pH 6.50, the adsorbent dose was 0.75g, and the adsorption capacity was 38.85mg/g when the adsorbent size was used under 35 mesh. In the above parameters, the maximum subtraction was 95%. Besides SEM, BET, FT-IR, adsorption has the Langmuir adsorption isotherm ($R^2=0.99$) and conforms to pseudo-second order ($R^2=0.99$) kinetics. In thermodynamic studies, it has been observed that adsorption is a self-propelled endothermic reaction. In the desorption studies, HCl and NaOH were used and the maximum yield was obtained as 4.04% and 0.88%, respectively. In line with these results, it was observed that there was no recovery in the adsorption process.

5. RESULTS

As a result, considering the factors such as the lack of economic value and easy availability of the *V. thapsus* plant, its use as an adsorbent was found to be suitable for MG dye adsorption. According to the researched data, the highest dye adsorption at room temperature was 304.00mg/L, pH 6.50, the adsorbent dose was 0.75g, and the adsorption capacity was 38.85mg/g when the adsorbent size was used under 35 mesh. In the above parameters, the maximum subtraction was 95%. Besides SEM, BET, FT-IR, adsorption has the Langmuir adsorption isotherm ($R^2=0.99$) and conforms to pseudo-second order ($R^2=0.99$) kinetics. In thermodynamic studies, it has been observed that adsorption is a self-propelled endothermic reaction. In the desorption studies, HCl and NaOH were used and the maximum yield was obtained as 4.04% and 0.88%, respectively. In line with these results, it was observed that there was no recovery in the adsorption process. The removal capacity of the VTL should be studied using real textile wastewater. The topic can be developed by working on real wastewater. VTL is a material suitable for combustion in cement plants after adsorption. In this way, it can be evaluated within the scope of zero waste production.

ACKNOWLEDGMENTS

This study was financially supported by Mersin University Scientific Research Projects Unit. (Project number: 2020-1-TP2-3849).

ABBREVIATIONS

C_0	: Initial dye concentration (mg/L)
C_e	: Concentration of solute remaining in solution without being adsorbed at Equilibrium (mg/L)
E_a	: Activation energy (kcal/mol)
k_0	: Activation energy constant
k_1	: First-order kinetic model rate constant (L/min)
k_2	: Second-order kinetic model rate constant (g/mg.min)
K_F	: Freundlich isotherm constant
n	: Adsorption density
R^2	: Correlation coefficient
T	: Temperature ($^{\circ}C$, K)
t	: Time
q_e	: Dye adsorbed per unit weight of adsorbent at equilibrium amount, (mg/g)
q_s	: unit of adsorber to form a complete monolayer on the surface
q_t	: Amount of dyestuff adsorbed at time t (mg/g)
ΔH	: Standard Enthalpy Change
ΔG	: Free Energy Entropy Change



ΔS	:	Entropy Change
V	:	Solution volume (L)
BET	:	Brunauer-Emmett-Teller Isotherm Model
FTIR	:	Fourier Transform Infrared Spectroscopy
SEM	:	Scanning Electron Microscope
HCl	:	Hydrochloric acid
NaOH	:	Sodium hydroxide
VTL	:	Verbascum Thapsus L.
MG	:	Malachite Green

CONFLICT OF INTEREST

The authors have no conflicts of interest to be disclosed.

FINANCIAL DISCLOSURE

This study was financially supported by Mersin University Scientific Research Projects Unit (Project number: 2020-1-TP2-3849).

DECLARATION OF ETHICAL STANDARDS

The authors of this article declare that the materials and methods used in this study do not require an ethical committee.

REFERENCES

- [1] Vakili, M., Rafatullah, M., Salamatinia, B., Abdullah, A.Z., Ibrahim, M.H., Tan, K.B., Gholami, Z., and Amouzgar, P., (2014). Application of chitosan and its derivatives as adsorbents for dye removal from water and wastewater: A review. *Carbohydrate Polymers*, 113:115-130.
- [2] Han, D., Zhao, H., Gao, L., Qin, Z., Ma, J., Han, Y., and Jiao, T., (2021). Preparation of carboxymethyl chitosan/phytic acid composite hydrogels for rapid dye adsorption in wastewater treatment. *Colloids and Surfaces A: Physicochemical and Engineering Aspects*, 628.
- [3] Garba, Z.N., Zhou, W., Lawan, I., Xiao, W., Zhang, M., Wang, L., Chen, L., and Yuan, Z., (2019). An overview of chlorophenols as contaminants and their removal from wastewater by adsorption: A review. *Journal of Environmental Management*, 241:59-70.
- [4] Lu, Y., Song, S., Wang, R., Liu, Z., Meng, J., Sweetman, A.J., Jenkins, A., Ferrier, R.C., Li, H., Luo, W., and Wang, T., (2015). Impacts of soil and water pollution on food safety and health risks in China. *Environment International*, 77:5-15.
- [5] Xiao, W., Jiang, X., Liu, X., Zhou, W., Garba, Z.N., Lavan, I., Wang, L., and Yuan, Z., (2021). Adsorption of organic dyes from wastewater by metal-doped porous carbon materials. *Journal of Cleaner Production*.
- [6] Lourenço, N., Novais, J., and Pinheiro, H., (2001). Effect of some operational parameters on textile dye biodegradation in a sequential batch reactor. *Journal of Biotechnology*, 89(2-3):163-174.
- [7] Salih, S.J., Kare, A.S., and Anwer, S.S., (2022). Adsorption of anionic dyes from textile wastewater utilizing raw corncob. *Heliyon*, 8(8):e10092.
- [8] Chen, Q., Zhang, Q., Yang, Y., Wang, Q., He, Y., and Dong, N., (2021). Synergetic effect on methylene blue adsorption to biochar with gentian violet in dyeing and printing wastewater under competitive adsorption mechanism. *Case Studies in Thermal Engineering*, 26:101099.
- [9] Gupta, V.K., Kumar, R., Nayak, A., Saleh, T.A., and Barakat, M., (2013). Adsorptive removal of dyes from aqueous solution onto



- carbon nanotubes: A review. *Advances in Colloid and Interface Science*, 1(193-194):24-34.
- [10] Wang, C.C., Juang, L.C., Hsu, T.C., Lee, C.K., Lee, J.F., and Huang, F.C., (2004). Adsorption of basic dyes onto montmorillonite. *Journal of Colloid and Interface Science*, 273(1):80-86.
- [11] Lee, C.K., Wang, C.C., Juang, L.C., Lyu, M.D., Hung, S.H., and Liu, S.S., (2008). Effects of sodium content on the microstructures and basic dye cation exchange of titanate nanotubes. *Colloids and Surfaces A: Physicochemical and Engineering Aspects*, 1(1-3):164-173.
- [12] Cheng, S., Zhao, S., Xing, B., Liu, Y., Zhang, C., and Xia, H., (2022). Preparation of magnetic adsorbent-photocatalyst composites for dye removal by synergistic effect of adsorption and photocatalysis. *Journal of Cleaner Production*, 348:131301.
- [13] Soh, E.Y., Lim, S.S., Chew, K.W., Phuang, X.W., Ho, W.M., Chu, K.Y., Wong, R.R., and Lee, L.Y., (2022). Valorization of spent brewery yeast biosorbent with sonication-assisted adsorption for dye removal in wastewater treatment. *Environmental Research*, 204:112385.
- [14] Ramutshatsha-Makhwedzha, D., Mavhungu, A., Moropeng, M.L., and Mbaya, R., (2022). Activated carbon derived from waste orange and lemon peels for the adsorption of methyl orange and methylene blue dyes from wastewater. *Heliyon*, 8(8):e09930.
- [15] Shoori, I.S., Jorabchi, M.N., Ghasemi, S., Golriz, M., Wohlrab, S., and Khonakdar, H.A., (2023). Advancements in wastewater Treatment: A computational analysis of adsorption characteristics of cationic dyes pollutants on amide Functionalized-MOF nanostructure MIL-53 (Al) surface. *Separation and Purification Technology*, 319:124081.
- [16] Wong, S., Ngadi, N., Inuwa, I.M., and Hassan, O., (2018). Recent advances in applications of activated carbon from biowaste for wastewater treatment: A short review. *Journal of Cleaner Production*, 175:361-375.
- [17] Khorram, A.G. and Fallah, N., (2018). Treatment of textile dyeing factory wastewater by electrocoagulation with low sludge settling time: Optimization of operating parameters by RSM. *Journal of Environmental Chemical Engineering*, 6(1):635-642.
- [18] Momina, K.A., (2023). Feasibility of the adsorption as a process for its large scale adoption across industries for the treatment of wastewater: Research gaps and economic assessment. *Journal of Cleaner Production*, 388:136014.
- [19] Davoodbeygi, Y., Askari, M., Salehi, E., and Kheirieh, S., (2023). A review on hybrid membrane-adsorption systems for intensified water and wastewater treatment: Process configurations, separation targets, and materials applied. *Journal of Environmental Management*, 335:117577.
- [20] Al-Gorair, A.S., (2019). Treatment of wastewater from cationic dye using eco-friendly nanocomposite: Characterization, adsorption and kinetic studies. *The Egyptian Journal of Aquatic Research*, 45(1):25-31.
- [21] Salahshoori, I., Jorabchi, M.N., Ghasemi, S., Golriz, M., Wohlrab, S., and Khonakdar, H.A., (2023). Advancements in wastewater Treatment: A computational analysis of adsorption characteristics of cationic dyes pollutants on amide Functionalized-MOF nanostructure MIL-53 (Al) surfaces. *Separation and Purification Technology*, 319:124081.
- [22] Aljohani, M.M., Al-Qahtani, S.D., Alshareef, M., El-Desouky, M.G., El-Bindary, A.A., El-Metwaly, N.M., and El-Bindary, M.A.,

- (2023). Highly efficient adsorption and removal bio-staining dye from industrial wastewater onto mesoporous Ag-MOFs. *Highly efficient adsorption and removal bio-staining dye from industrial wastewater onto mesoporous Ag-MOFs*. *Process Safety and Environmental Protection*, 172:395-407.
- [23] Liu, Z., Huang, X., Miao, Y., Gao, B., Shi, Y., Zhao, J., and Tan, S.H., (2022). Eggplant biomass based porous carbon for fast and efficient dye adsorption from wastewater. *Industrial Crops and Products*, 187(B):115510.
- [24] Dey, P., Mahapatra, B., Juyal, V., Pramanick, B., Negi, M., Paul, J., and Singh, S., (2021). Flax processing waste - A low-cost, potential biosorbent for treatment of heavy metal, dye and organic matter contaminated industrial wastewater. *Industrial Crops and Products*, 174:114195.
- [25] Laverde, M.P., Salamanca, M., Diaz-Corrales, J.D., Flórez, E., Agredo, J.S., and Torres-Palma, R.A., (2021). Understanding the removal of an anionic dye in textile wastewaters by adsorption on ZnCl₂ activated carbons from rice and coffee husk wastes: A combined experimental and theoretical study. *Journal of Environmental Chemical Engineering*, 9(4):105685.
- [26] Özacar, M. and Şengil, I., (2004). Two-stage batch sorber design using second-order kinetic model for the sorption of metal complex dyes onto pine sawdust. *Biochemical Engineering Journal*, 21(1):39-45.
- [27] Yadav, J., Sahu, O., and Marwah, H., (2022). Bioadsorption of dye from textile effluent with surface response methodology. *Materialstoday proceedings*, 68(4):937-942.
- [28] Besegatto, S.V., Martins, M.L., Lopes, T.J., Adriano, A., and Silva, A.D., (2021). Multivariate calibration as a tool for resolution of color from mandarin peel and dyes in aqueous solution for bioadsorption studies. *Journal of Environmental Chemical Engineering*, 9(1):104605.
- [29] Sahu, O. and Singh, N., (2019). 13 - Significance of bioadsorption process on textile industry wastewater. *The Impact and Prospects of Green Chemistry for Textile Technology*, 367-416.
- [30] Obayomi, K.S., Lau, S.Y., Danquah, M.K., Zhang, J., Chiong, T., Meunier, L., Gray, S.R., and Mahmudur, M.R., (2023). Green synthesis of graphene-oxide based nanocomposites for efficient removal of methylene blue dye from wastewater. *Desalination*, 564:116749.
- [31] El-Kammah, M., Elkhatib, E., Gouveia, S., Cameselle, C., and Aboukila, E., (2022). Cost-effective ecofriendly nanoparticles for rapid and efficient indigo carmine dye removal from wastewater: Adsorption equilibrium, kinetics and mechanism. *Environmental Technology & Innovation*, 28:102595.
- [32] Ahmad, R. and Kumar, R., (2010). Adsorption studies of hazardous malachite green onto treated ginger waste. *Journal of Environmental Management*, 91(4):1032-1038.
- [33] Bekçi, Z., Özveri, C., Yoldaş, S., and Yurdak, K., (2008). Sorption of malachite green on chitosan bead. *Journal of Hazardous Materials*, 154(1-3):254-261.
- [34] Weldegebrieal, G.K., (2020). Photocatalytic and antibacterial activity of CuO nanoparticles biosynthesized using *Verbascum thapsus* leaves extract. *Optik*, 204.
- [35] Prakash, V., Rana, S., and Sagar, A., (2016). Studies on Antibacterial Activity of *Verbascum*. *Journal of Medicinal Plants Studies*, 4(3):101-104.



- [36] Okasha, Y.M., Fathy, F.I., Soliman, F.M., and Fayek, N.M., (2023). The untargeted phytochemical profile of *Verbascum thapsus* L. with potent antiviral, antibacterial and anticancer activities. *South African Journal of Botany*, 156:334-341.
- [37] Elemike, E.E., Onwudiwe, D.C., and Mkhize, Z., (2016). Eco-friendly synthesis of AgNPs using *Verbascum thapsus* extract and its photocatalytic activity. *Materials Letters*, 185:452-455.
- [38] Saleh, M., Işık, Z., Aktaş, Y., Arslan, H., Yalvaç, M., and Dizge, N., (2021). Green synthesis of zero valent iron nanoparticles using *Verbascum thapsus* and its Cr (VI) reduction activity. *Bioresource Technology Reports*, 13.
- [39] Yadav, J. and Sahu, O., (2023). Malachite green dye purification from effluent using synthesized ceramic clay: Characterisation; optimization and scale up. *Ceramics International*, 49(15):24831-24851.
- [40] Hashem, A.A., Mahmoud, S.A., Geioushy, R.A., and Fouad, O.A., (2023). Adsorption of malachite green dye over synthesized calcium silicate nanopowders from waste materials. *Materials Science and Engineering: B*, 295.
- [41] Wolska, J., Muńko, M., EL Siblani, H., Igor, T., Frankowski, M., Sz wajca, A., Walkowiak-Kulikowska, J., El-Roz, M., and Wolski, L., (2023). The influence of cross-linking density on the efficiency of post-synthetic sulfonation of hyper-cross-linked polymers and their adsorption capacity for antibiotic pollutants. *Journal of Environmental Chemical Engineering*, 11(5):110429.
- [42] Onu, C.E., Nwabanne, J.T., Ohale, P.E., and Asadu, C.O., (2021). Comparative analysis of RSM, ANN and ANFIS and the mechanistic modeling in eriochrome black-T dye adsorption using modified clay. *South African Journal of Chemical Engineering*, 36:(24-42).